RSC Sustainability

ROYAL SOCIETY OF CHEMISTRY

PAPER

View Article Online
View Journal

Cite this: DOI: 10.1039/d6su00192k

Biodiesel production under a microwave-assisted approach using a glycerol-derived Zn bifunctional catalyst

Michelle Pains Duarte,[ab] Luis Páramo,[ab] Tashiah Roper-Mungal[ab] and Rafik Naccache *[ab]

Biodiesel production still relies heavily on homogeneous catalysts and edible oils, which leads to costly production and purification steps. Heterogeneous bifunctional catalysts have emerged as promising alternatives as they can be easily recovered and reused, in addition to tolerating low-grade feedstocks. Moreover, biodiesel production generates a substantial amount of crude glycerol as a byproduct, which creates a crucial need for valorisation strategies. Herein, to overcome these challenges, a zinc oxide-glycerol-based material was synthesized and employed as a bifunctional catalyst for the conversion of acidified corn oil into biodiesel *via* a microwave-assisted approach. Physicochemical characterization revealed a flower-like mesoporous structure and the presence of ZnO as the main active phase. Reaction parameters, including oil-to-methanol molar ratio, catalyst loading, temperature, and reaction time, were optimized to determine conditions that maximize conversion efficiency, achieving the highest conversion of 94.5% at 150 °C for 1.5 hours using a 5 wt% catalyst loading and a 1 : 24 oil-to-methanol molar ratio. Furthermore, reusability studies showed that the material remains stable for up to five reaction cycles. Our findings highlight the potential of using glycerol as a precursor for the synthesis of heterogeneous catalysts and offer a circular and economically viable alternative for biodiesel production, rendering it more sustainable.

Received 2nd April 2026
Accepted 3rd May 2026

DOI: 10.1039/d6su00192k

rsc.li/rscsus

Sustainability spotlight

Biodiesel represents a promising alternative in the transition towards renewable energy. However, its production still faces some challenges related to the heavy reliance on refined oils and the large amount of crude glycerol generated during the process. This study converts glycerol into a bifunctional ZnO-carbon catalyst capable of performing transesterification and esterification simultaneously, allowing the production of biodiesel from low-grade feedstocks. This work promotes a circular economy by transforming glycerol, the main byproduct of the process, into a reusable catalyst and enables the production of biodiesel from non-refined oils, reducing the dependence on refined edible oils. As such, it supports UN Sustainable Development Goals 7 (Affordable and Clean Energy), 2 (Zero Hunger), 9 (Industry, Innovation and Infrastructure), 12 (Responsible Consumption and Production), and 13 (Climate Action), and contributes to a more sustainable biodiesel production and the valorization of glycerol.

Introduction

The Industrial Revolution marked the transition from traditional energy sources such as wood and charcoal to coal, oil, and gas. These hydrocarbon-rich resources originated from the accumulation of decomposed algae, bacteria, and plant matter within the Earth's crust.[1] Upon combustion, substantial amounts of energy are released alongside emission of undesirable gaseous byproducts, including carbon dioxide, methane, nitrous oxide, and sulfur dioxide.[1,2] Over the last century, fossil fuels have been the foundation of global energy systems, meeting the energy demands of economic and population growth.[3] However, their extensive use has been a main contributor to escalating greenhouse gas emissions and global warming. According to the 2025 International Energy Agency[4] report, global energy-related CO_2 emissions reached a record high of 37.8 gigatons in 2024, primarily driven by natural gas and coal emissions, coinciding with the warmest year on record. With a continuous upward trend for global fossil fuel consumption and reserves projected to sustain energy production for as little as another 30 to 150 years at current rates, reliance on these finite resources is both harmful to the environment and unsustainable.[3,5,6] This has instigated the urgent need to transition toward clean, renewable energy sources, where solar energy, geothermal energy, wind power,

[a]Department of Chemistry and Biochemistry and the Centre for NanoScience Research, Concordia University, Montreal, QC, H4B 1R6, Canada. E-mail: rafik.naccache@concordia.ca

[b]Quebec Centre for Advanced Materials, Department of Chemistry and Biochemistry, Concordia University, Montreal, QC, H4B 1R6, Canada

hydropower, and biofuels, particularly biodiesel, are amongst the most promising.[2,7]

Biodiesel is a renewable alternative to fossil-fuel-derived diesel, sharing similar physicochemical properties. Studies have shown compatibility with existing fuel systems,[8–10] enhanced lubricity and combustion efficiency,[10] greater biodegradability,[11] and reduced CO, CO_2, NO, and SO_2 emissions[12] compared to conventional diesel. In chemical terms, biodiesel consists of long-chain fatty acid mono-alkyl esters (FAMEs) formed *via* reversible (trans)esterification reactions in the presence of a catalyst, requiring optimized reaction conditions to drive ester formation. It is produced from organic feedstocks including algae, animal fats, and oils typically classified as edible (*e.g.*, canola, soybean, palm) or non-edible and waste-derived oils (*e.g.*, Jatropha, waste cooking oil).[13–16] The choice of feedstock largely determines the cost and sustainability of the process, while the catalyst influences reaction efficiency.

Industrial processes conventionally utilize homogeneous catalysts such as H_2SO_4, or more commonly, strong bases like NaOH and KOH, which show high conversions under moderate conditions.[17] However, ion dissociation leads to saponification with high acidity feedstocks, extensive purification steps, and difficulties in product separation.[14,15,17] Hence, current biodiesel production often relies on low free fatty acids (FFA) edible oils, raising concerns about its conflicting involvement in both energy and food markets.[13,18] These notable limitations, with consequent elevated process costs, present operational drawbacks that hinder its widespread adoption.[19] Heterogeneous catalysts have emerged as an alternative to circumvent these obstacles, simplifying product separation, reducing water-intensive purification, and allowing the use of waste-derived precursors from domestic and industrial activities.[17] Numerous catalysts of both acidic and alkaline nature have been studied, namely alkali metal oxides,[20] transition metal oxides,[8,21] zeolites,[22,23] carbon-based materials,[13,24,25] and bio-waste-derived materials.[26,27] However, alkaline heterogeneous catalysts remain intolerant to moisture and FFA, limiting their application to refined oils, whilst acidic heterogeneous catalysts, although efficient in catalyzing esterification reactions, suffer from low reaction rates in transesterification.[28]

More recently, researchers have explored the design of bifunctional catalysts, such as ionic liquids,[29,30] heteropoly acids,[31] and mixed metal oxides,[32–34] which combine acidic and basic active sites, enabling the simultaneous esterification of free fatty acids (FFA) and transesterification of triglycerides.[35,36] This allows both high-FFA waste oils and edible oils to be converted to biodiesel in a single step, eliminating pretreatment steps to reduce acidity and supporting greater feedstock flexibility and sustainability.[35,36]

Nonetheless, most of these bifunctional catalysts rely on complex and expensive synthetic routes. As such, biomass-derived carbon materials have emerged as an attractive choice for the development of these catalysts, owing to their eco-friendly, affordable, and easy synthesis, supporting a shift toward greater sustainability.[26,37–39] These materials have garnered significant interest as heterogeneous catalysts owing to their porous structure, high surface area, chemical stability, strong adsorption, and their surface functionalization with specific chemical groups or elements to introduce active sites for the transesterification of feedstocks.[37,40,41] Akhabue *et al.*[42] reported ≥92% conversion of neem oil with 4.4% FFA using a bifunctional catalyst made from corncobs and poultry droppings. Gnanaserkhar *et al.*[43] investigated the conversion of chicken fat oil, with 16.83% FFA, using a bifunctional carbon-based catalyst made from coconut shell doped with CeO_2, achieving a conversion of 93%. Recently, Maleki *et al.*[44] explored an activated carbon doped with zinc and nickel oxide as a bifunctional catalyst for the conversion of dairy industry waste oil into biodiesel, obtaining conversions >97%.

The growing emphasis on waste reduction and energy efficiency highlights crude glycerol, an abundant byproduct accounting for roughly 10% of total biodiesel output, as a valuable renewable resource.[45] Its accumulation from continuous global expansion poses economic and experimental challenges due to the energy-intensive purification required before conventional use. However, crude glycerol can be valorized into high-value chemicals and heterogeneous catalysts, enabling its reuse within the biodiesel process.[46] An investigation by Prabhavathi Devi *et al.*[47] reported 99% conversion of palmitic acid using a glycerol-derived carbon-based catalyst. Hazmi *et al.*[48] obtained conversions exceeding 96.7% from palm fatty acid distillate (PFAD) using sulfonated glycerol carbon-based catalysts. These studies reveal the potential in exploiting crude glycerol as a renewable catalyst with the added advantage of reducing waste accumulation and enhancing the overall sustainability and feasibility of biodiesel production.

Another parameter that affects the sustainability of the process is the conventional heating methods employed, which are energy-demanding, promote non-uniform heating, and often require longer reaction times. As such, microwave-assisted reaction emerged as a promising alternative. Microwave irradiation promotes direct and uniform heating within the reaction media, consequently reducing reaction times and energy consumption. It also renders better yields and selectivity under milder conditions, lowering the generation of byproducts and waste.[49,50] Therefore, a microwave-assisted approach is generally considered a greener method, since it addresses some of the 12 Principles of Green Chemistry, improving the sustainability of the whole process. Indeed, several studies have reported the synthesis of biodiesel through a microwave-assisted approach, proving the efficiency of this method.[51–54]

Herein, this work presents a novel and sustainable approach for biodiesel production based on the valorization of glycerol into a bifunctional catalyst. Although ZnO-based materials have been widely reported for biodiesel production, they often rely on complex and multistep synthetic routes. Therefore, this study explores a simple one-pot synthesis of a glycerol-derived Zn-based heterogeneous catalyst, enabling the simultaneous formation of the carbon matrix and the *in situ* generation of ZnO.

Zinc acetate and urea were combined with pure glycerol, pyrolyzed, and used as a bifunctional catalyst for the simultaneous transesterification and esterification of acidified corn oil (10 wt% FFA) *via* a microwave-assisted reaction. Unlike previous glycerol-based catalysts reported in the literature, which were

mainly based on sulfonated materials and applied to the esterification reaction, this work presents a glycerol-based catalyst capable of converting low-grade oils in a single step.

Moreover, the effects of key reaction parameters, including oil-to-methanol ratio, catalyst loading, reaction time, and temperature, were examined to optimize biodiesel conversion. Additionally, the catalyst was comprehensively characterized to elucidate its surface chemistry and clarify its role in the reaction. The findings highlight a novel approach to valorize surplus glycerol by converting it into a bifunctional catalyst, and proving it to be a promising substitute for conventional homogeneous-catalyzed systems. Furthermore, the use of the microwave-assisted approach improves the sustainability of the process, reducing reaction times and energy demands. Therefore, this study provides a more sustainable and economically viable route for biodiesel production, addressing the main challenges faced by the current processes.

Experimental

Materials

Urea (>99%) and oleic acid (technical grade, 90%) were purchased from Sigma Aldrich. Glycerol (>99%), zinc acetate dihydrate (98–101%), methanol (99%), and acetone (99.6%) were purchased from Fisher Scientific. Food-grade corn oil was purchased from a local grocery store. All the chemicals were used as received, without further purification.

Catalyst preparation

The glycerol-based material was prepared following the protocol described by Wang *et al.*,[55] with slight modifications. Briefly, 3 g of zinc acetate and 1 g of urea were added to 20 mL of glycerol, and ground together in a mortar and pestle. The mixture was then transferred to alumina combustible boats and carbonized under argon, for 1 h, at 800 °C using a heating rate of 5 °C min^{-1}. After the reaction, the solid obtained was milled into a fine powder and labelled Gly–Zn.

Catalyst characterization

Scanning electron microscopy (SEM) and energy dispersive X-ray spectroscopy (EDS) measurements were obtained using a Phenom ProX Desktop instrument. Powder X-ray diffraction (PXRD) pattern was acquired using a Rigaku MiniFlex 6G diffractometer (Cu Kα source; $\lambda = 1.54$ Å), ranging from 10° 2θ to 80° 2θ. A TGA Q500 analyser was employed to perform thermogravimetric analysis. The sample was heated under an oxidizing atmosphere from 25 to 900 °C at a rate of 10 °C min^{-1}. Brunauer–Emmett–Teller (BET) surface area and BJH (Barrett–Joyner–Halenda) pore size distribution were determined by N_2 sorption isotherms collected at 77 K on a Micromeritics TriStar II Plus instrument. Prior to the analysis, the sample was activated at 100 °C for 20 h under vacuum.

Catalytic performance in esterification-transesterification

The catalytic activity of Gly–Zn was evaluated for the simultaneous transesterification and esterification of an acidified corn oil (10% FFA). The acidified oil was characterized in terms of moisture content, acid value, saponification value, and average molecular mass as shown in Table 1.

The reactions were carried out using a microwave-assisted solvothermal approach in a MARS 6 CEM Digestion Microwave (800 W). Briefly, a known amount of Gly–Zn (1–7 wt% of oil) was added to 2 mL of the acidified corn oil and methanol (1 : 9–1 : 36 oil-to-methanol molar ratio). The reaction mixture was then heated at temperatures ranging from 75 °C to 150 °C, and reaction times ranging from 30 minutes to 2 h. At the end of the reaction, the system was cooled down to ambient temperature and centrifuged at 10 000×*g* for 5 minutes in order to separate the phases, followed by the evaporation of the top layer, methanol, in a 65 °C oven. All the reactions were carried out in triplicate to ensure reproducibility. The final product was then characterized, and the conversion was quantified through ^{1}H NMR spectroscopy on a Bruker Fourier-300 MHz using eqn (1):[58]

$$C = \frac{2 \times A_{CH_3}}{3 \times A_{CH_2}} \times 100 \quad (1)$$

where A_{CH_3} represents the integration area ascribed to the methoxy protons present in the methyl ester at 3.66 ppm, and A_{CH_2} is ascribed to the integration area of α-methylene protons at 2.3 ppm present in the triglyceride and methyl ester (Fig. S1).

Results and discussion

Catalyst characterization

SEM analysis revealed a flower-like morphology, composed of stacked nanosheets (Fig. 1a and b). This finding aligns with studies reported by Wang *et al.*[55] and Chang *et al.*,[59] which demonstrated that the carbonization of glycerol in the presence of zinc salts led to the formation of sheet-like carbon structures similar to the ones observed in this study.

Glycerol was used as a carbon precursor but also as a small molecular organic solvent (SMOS) for the synthesis of the carbon-based catalyst. The formation of the material relies on the synergistic interaction among the precursors. According to Wang *et al.*[55] and Wu *et al.*,[60] zinc acetate acts as a stabilizer, where the Zn^{2+} ions coordinate with the oxygen and nitrogen atoms of glycerol and urea, forming thermally stable polymeric intermediates and preventing their volatilization at elevated temperatures. Moreover, urea acts not only as a nitrogen source, promoting *in situ* doping, but it also neutralizes acidic byproducts that evolve from the decomposition of glycerol

Table 1 Physicochemical properties of the acidified corn oil (10 wt% FFA) used as feedstock

Property	Value	Ref.
Acid value (mg KOH per g oil)	20.05	56
Saponification value (mg KOH per g oil)	190.82	56
Moisture content (wt%)	0.18	56
Average molecular weight (g mol^{-1})	985.54	57
Density (kg m^{-3}) at 21 °C	889.9	56

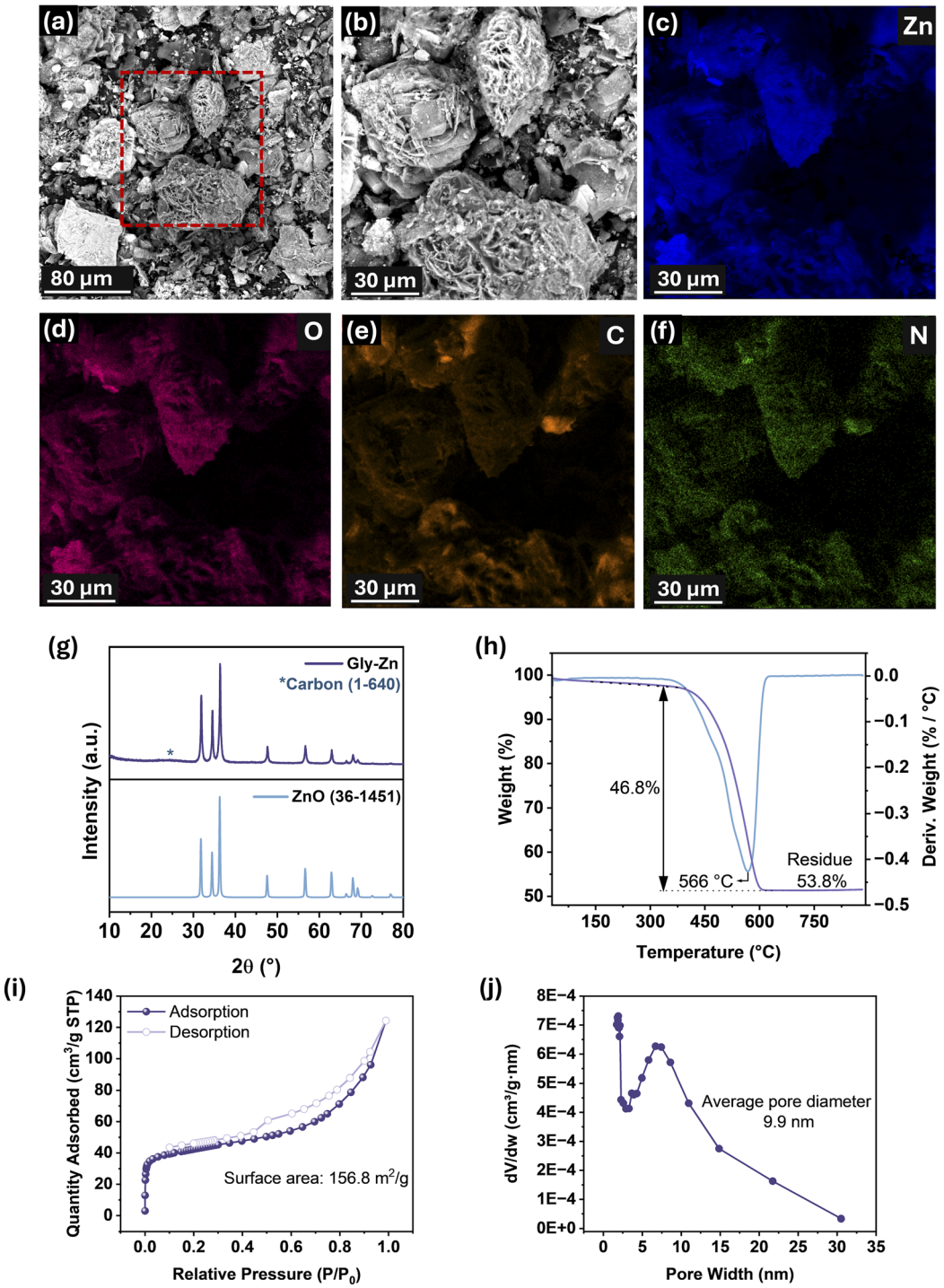

Fig. 1 (a and b) SEM images of Gly–Zn, revealing a flower-like morphology, composed of stacked nanosheets; (c–f) EDS mapping confirming the uniform distribution of zinc (blue), oxygen (pink), carbon (orange), and nitrogen (green); (g) PXRD pattern of Gly–Zn displays characteristics reflection of zinc oxide and a weak and broad vibration characteristic of amorphous carbon; (h) TGA and dTG curves of Gly–Zn showing one mass event associated with the oxidation of the carbon matrix. (i) N_2 adsorption/desorption isotherms of Gly–Zn evidence a type IV isotherm characteristic of mesoporous materials, with type H3 hysteresis; (j) Pore size distribution of Gly–Zn obtained *via* the BJH method.

owing to the release of ammonia during the carbonization process.[55]

EDS analysis confirmed the uniform distribution of Zn, C, O, and N throughout the surface of the material (Fig. 1c–f). The presence of nitrogen corroborates the *in situ* doping of urea described previously, while the simultaneous presence of zinc and oxygen indicates the formation of ZnO within the carbonaceous matrix. The incorporation of ZnO throughout the carbon material, according to Wang *et al.*,[55] can be described by the decomposition of zinc acetate into ZnO, releasing CO_2 and

acetone (eqn (2)), but also by the decomposition of a glycerin-zinc intermediate, forming ZnO and the carbonaceous structure shown in eqn (3).

$$Zn(CH_3COO)_2 \rightarrow ZnO + CO_2 + CH_3COCH_3 \quad (2)$$

$$Zn_x(CH_3H_{5-z}O_3)_y \rightarrow xZnO + 3yC + (3y - x)H_2O \quad (3)$$

PXRD analysis of Gly–Zn was performed (Fig. 1g), revealing characteristic diffraction peaks at 31.8°, 34.5°, and 36.3° 2θ attributed to the (100), (002), and (101) planes of the hexagonal wurtzite structure of ZnO (JCPDS 36-1451), respectively.[61] Moreover, a broad and weak diffraction peak at ~22° 2θ ascribed to graphite (JCPDS-1-640) is observed, indicating an amorphous structure. This disorder is likely associated with the presence of ZnO within the carbonaceous matrix, which can inhibit the graphitization of the carbon sheets.[62] These findings corroborate the EDS results, which indicated a uniform distribution of Zn, O, and C. Moreover, the Debye–Scherrer equation (eqn (4)) was used to determine the average crystallite size of Gly–Zn:

$$D = \frac{K\lambda}{\beta \cos \theta} \quad (4)$$

where D is the crystallite size, K is the Scherrer constant, λ is the X-ray wavelength, β is the full width at half maximum, and θ is the Bragg angle. The crystallite size was calculated for each diffraction peak, and the average size was determined to be 25.3 nm.

The thermal stability and the relative concentrations of ZnO and the carbon moiety were investigated by TGA, as shown in Fig. 1h. The thermogram indicates that the material remains thermally stable up to 480 °C, confirming its suitability for the temperature range used in biodiesel reactions.[63,64] Furthermore, a single mass loss event of ~46.8% with a maximum decomposition temperature of 566 °C was observed and attributed to the oxidation of the carbonaceous matrix, with a residual mass of 53.2%, ascribed to the ZnO fraction of the material.[65]

The textural properties of the material were investigated by N_2 adsorption–desorption isotherms, as shown in Fig. 1i and j. The material presented a type IV isotherm, typical of mesoporous materials, with an H3-type hysteresis, characteristics of plate-like aggregates that create slit-like voids.[66] These findings align with the SEM results, which revealed a morphology composed of stacked carbon sheets. Moreover, the material exhibited a specific surface area of 156.8 $m^2\ g^{-1}$ and an average pore diameter of 9.9 nm. These results indicate that the material is suitable for biodiesel reactions, as its pore size facilitates the diffusion of triglycerides and oleic acid to the active sites within the carbon matrix.[67]

In ZnO-based materials, Zn^{2+} metallic centers and oxygen vacancies act as Lewis acid sites, while lattice oxygen (O^{2-}) and surface hydroxyl groups provide Lewis basic sites, promoting a synergetic acid–base feature. The bifunctional nature of ZnO-based materials has been widely reported and experimentally supported through NH_3-TPD, CO_2-TPD, and pyridine-FTIR, showing acidity and basicity densities ranging from 0.03 to 4.9 mmol g^{-1} and 0.01 to 3.0 mmol g^{-1}, respectively.[68–74] Similar to this study, Wang *et al.*[75] synthesized ZnO-based catalysts with nitrogen-rich precursors and reported a total acidity up to 0.04 mmol g^{-1} and a total basicity up to 0.01 mmol g^{-1}. Thus, based on the physicochemical properties of the material, and considering the potential of ZnO to act as a bifunctional catalyst, owing to the presence of acidic and basic sites,[76] Gly–Zn was investigated as a heterogeneous catalyst for the simultaneous transesterification and esterification reactions.

Catalytic performance under different reaction approaches

The catalytic performance of Gly–Zn was evaluated using three different reaction approaches to assess the effect of the reaction nature on the catalytic activity and on the conversion, while considering the energetic efficiency of the process (Fig. 2 and S2). The reactions were carried out using an acidified corn oil containing 10% FFA as feedstock, under the conditions of an oil-to-methanol molar ratio of 1 : 36, and a catalyst loading of 5 wt%. The first approach investigated was conventional heating, using a crimped glass vial heated in an oil bath. The reaction was performed at 90 °C for 3 hours, reaching a conversion of 21%. Conventional heating methods are known to create temperature gradients and non-uniform heating as they rely on convection and conduction phenomena,[77,78] in addition to consuming a considerable amount of energy. Thus, in order to overcome this limitation and improve the conversion rate, a solvothermal reaction was carried out using an autoclave with a Teflon reactor under the same conditions. Nonetheless, a similar conversion of 20% was achieved. Therefore, a reaction at a higher temperature, 150 °C, was performed, while maintaining the other conditions constant. A significant improvement in conversion was observed, as it increased to 98%. This improvement is likely associated with the fact that pressurized solvothermal systems allow a more uniform temperature distribution, enhanced mass and heat transfer, and consequently, a higher reaction rate owing to higher temperatures and pressure.[79–81]

Although the solvothermal system achieved almost complete conversion, it required high temperature for a prolonged time, which renders it a non-energy-efficient process. As such, a microwave-assisted solvothermal reaction was investigated to reduce the reaction temperature and/or time. Microwave-assisted reactions have attracted attention lately as they allow rapid and more uniform heating and consequently reduce the reaction time and improve yields.[77,78,82] A low conversion of 1.6% was obtained when the reaction was performed under 1 : 36 oil-to-methanol, 5 wt% catalyst loading, 90 °C, and 30 minutes. However, increasing the temperature to 150 °C led to a conversion of 49%. Thus, to further improve the conversion, a reaction was performed for 1 hour, keeping the other conditions constant, resulting in 95% biodiesel conversion. In comparison, a non-assisted microwave solvothermal reaction was carried out under the same conditions, reaching a conversion of 81%. These findings demonstrated that microwave-assisted systems enhance catalytic activity and the energy efficiency of the process, allowing high conversions within shorter reaction times.[83]

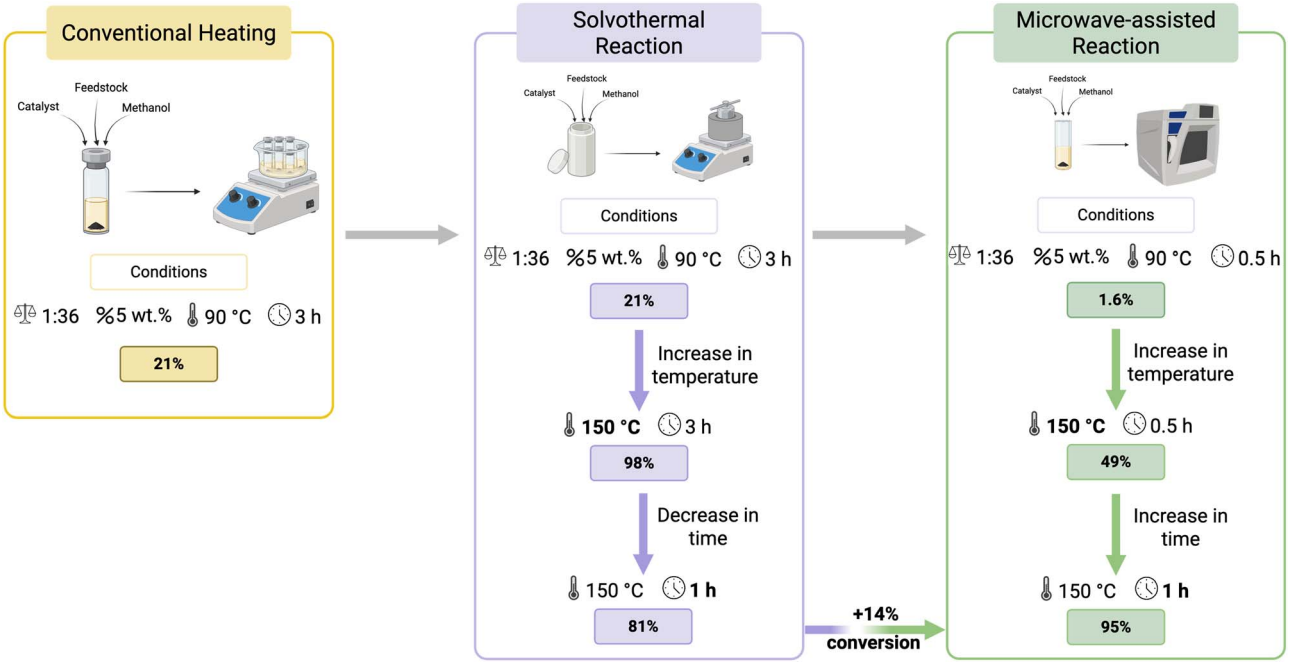

Fig. 2 Comparison between different reaction approaches to evaluate the catalytic performance of Gly–Zn. The microwave-assisted method demonstrated superior efficiency, achieving a 95% conversion at 150 °C in 1 h, representing a 14% increase compared to the solvothermal method under identical conditions.

Therefore, the one variable at a time (OVAT) method was employed to optimize the reaction parameters for the simultaneous (trans)esterification of the acidified oil using the microwave-assisted solvothermal approach.

Reaction optimization under microwave-assisted conditions

Among the different parameters that affect the biodiesel synthesis, the oil-to-methanol molar ratio is one of the most critical, as an excess of methanol is essential in order to displace the equilibrium towards the product formation.[84–86] Higher molar ratios are often required for bifunctional systems to ensure the efficient conversion of FFAs and triglycerides. However, an excessive amount of methanol can lead to the emulsification of glycerol and FAMEs, reducing the overall conversion and increasing the process costs.[86,87] Thus, it is crucial to determine the optimal oil-to-methanol molar ratio. Reactions were performed using molar ratios ranging from 1 : 9 to 1 : 36, while the other parameters, catalyst loading, temperature, and time, were kept constant (5 wt%, 150 °C, and 1 h). No significant changes were observed when the molar ratio varied from 1 : 36 to 1 : 24, achieving a 92.1% for the latter. However, a progressive decrease in conversion was observed when the oil-to-methanol ratio was reduced to 1 : 18 and 1 : 9, achieving conversions of 87.4% and 71.1%, respectively (Fig. 3a and S3). Therefore, 1 : 24 was selected as the optimal molar ratio for the subsequent optimizations. Studies reported in the literature for bifunctional catalysts show that the molar ratio can vary from 1 : 6 to 1 : 60,88 confirming the efficiency of the glycerol-based catalyst at this ratio.

Subsequently, the catalyst loading was evaluated (Fig. 3b and S4). The amount of catalyst directly affects the reaction rate and conversion. An insufficient loading results in low conversion due to a lack of active sites, while an excessive amount can cause emulsification and increase mass-transfer resistance.[84,89] The reactions were carried out with catalyst loadings ranging from 1 to 7 wt%, maintaining all other parameters constant (1 : 24 molar ratio, 150 °C, and 1 h). The highest conversion was achieved at the catalyst loading of 5 wt%, with a conversion of 92.1%. A slight decrease was observed at 3 wt% (90.2%), with a more pronounced decrease at 1 wt% (82%). This result indicates that a 5 wt% catalyst loading provides enough active sites to promote the (trans)esterification reaction, while lower amounts are insufficient. In addition, above 5 wt%, a slight decrease in conversion (87%) was observed, which is likely associated with limited diffusion between the catalyst and the reaction medium. As such, 5 wt% was selected as the optimal catalyst loading. Ihsan *et al.*[90] observed similar behaviour when they applied a K_2O/ZrO_2–Bi_2O_3 bifunctional catalyst for the conversion of wild olive seed oil. A maximum conversion was observed at 4 wt%, while a slight decrease was observed above and below this amount, which was associated with the insufficient number of active sites at lower loadings and with the excess of catalyst increasing the viscosity of the reaction medium.[90]

Transesterification and esterification reactions are endothermic, indicating that an increase in temperature favours the formation of FAMEs.[81] Higher temperatures facilitate the activation of carbonyl groups and, consequently, the nucleophilic attack. Moreover, they reduce the viscosity of the medium, enhancing mass transfer and increasing the frequency of collisions between molecules.[81,91] Therefore, to study the effect of temperature, reactions were conducted at 75 °C, 100 °C, 125 °

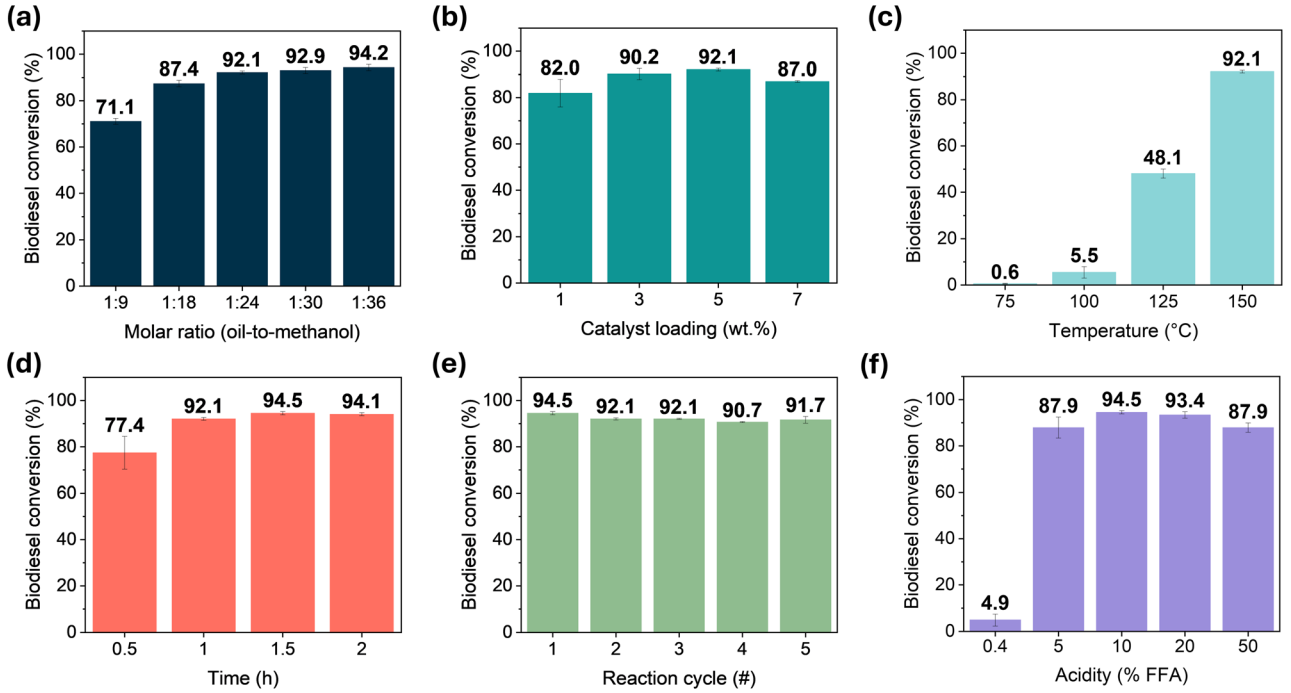

Fig. 3 Reaction optimization of (a) molar ratio, (b) catalyst loading (wt%), (c) temperature (°C), and (d) reaction time. (e) Reusability test of Gly–Zn as a bifunctional catalyst for the simultaneous transesterification and esterification reactions of acidified corn oil (10% FFA). (f) Effect of FFA content on biodiesel conversion using Gly–Zn as a catalyst under conditions of 1 : 24 oil-to-methanol ratio, 5 wt% catalyst loading, 150 °C for 1.5 h.

C, and 150 °C, while oil-to-methanol molar ratio, catalyst loading, and time were kept at 1 : 24, 5 wt%, and 1 h (Fig. 3c and S5). A gradual increase in conversion was observed as the reaction temperature increased. At 75 °C and 100 °C, low conversions of 0.6% and 5.5% were achieved, respectively, indicating that at these temperatures the energy supplied was insufficient to promote adequate diffusion of the reaction medium and the activation of, and nucleophilic attack on, the carbonyl groups. A significant increase was observed at 125 °C, reaching 48.1%, suggesting that at this temperature, mass transfer and carbonyl activation were enhanced. Further increase in conversion was observed at 150 °C, reaching 92.1%, confirming that elevated temperatures provide appropriate energy to improve diffusion, reduce viscosity, and promote the activation of the carbonyl groups of the FFAs and triglycerides. Thus, the optimal temperature was determined to be 150 °C. Wang *et al.*[92] studied a bifunctional catalyst for the conversion of *Jatropha curcas* oil, and observed the same trend, in which the conversion gradually increased as the temperature was raised from 85 °C to 125 °C, reaching its maximum at 125 °C.

Lastly, the effect of the reaction time was evaluated (Fig. 3d and S6). A suitable reaction time is essential to achieve optimal conversion of triglycerides and FFAs, given that the reaction proceeds in consecutive steps. Short reaction times may result in incomplete conversion, while prolonged times can favour reverse and/or side reactions.[81,84,93] Reactions were performed under the conditions of a 1 : 24 molar ratio, 5 wt% catalyst loading, 150 °C, and reaction times ranging from 30 minutes to 2 h. The lowest conversion, 77.4%, was achieved at 30 minutes, suggesting that the conversion was incomplete owing to the limited time available for effective interaction between the reactants and catalytic sites. The conversion rose to 92.1% as the reaction time increased to 1 h, with a slight increase to 94.5% when extended to 1.5 h. However, a further increase in time did not lead to higher conversions, as 94.1% was obtained after 2 h of reaction. These results indicate that the reaction approached its equilibrium under these conditions and that reaction times longer than 1.5 h did not enhance catalytic performance.[94] Moreover, these findings demonstrate that further extending the time offers no tangible improvement in conversion and unnecessarily raises the energy consumption of the process.[83] Therefore, the optimal time was determined to be 1.5 h.

Thus, the optimal conditions were determined as 1 : 24, 5 wt%, 150 °C, and 1.5 h. These conditions are notable considering that the catalyst is derived from glycerol, the main byproduct of biodiesel production. Consequently, the use of this material contributes to the valorisation of crude glycerol, promoting a more sustainable process and supporting the circular economy. Moreover, the use of the microwave-assisted approach proves to be a greener and more sustainable alternative for biodiesel production, owing to its high efficiency in heating the reaction medium and reducing reaction time. Conversions higher than 90% were achieved within 1 h, while conventional heating processes typically require several hours to reach comparable results.

A comparison with previously reported ZnO-based catalysts in the literature is shown in Table 2. Although some studies achieved high conversions under milder conditions, they often

relied on refined feedstocks, such as soybean and sunflower oils. However, catalysts capable of converting waste or acidic oils required longer reaction times or higher temperatures. Thus, Gly–Zn proved to be promising, as it was able to achieve a conversion of 94.5% of an acidic oil (10 wt% FFA) under the conditions of 1 : 24 molar ratio, 5 wt%, 150 °C, and 1.5 h. Moreover, the Gly–Zn catalyst was easily synthesized using a simple one-pot synthesis derived from glycerol and zinc acetate. This approach avoids complex and multi-step routes often employed for ZnO-based materials, and allows the use of the reaction byproduct, rendering the process simpler and more efficient.

Reusability study

Following the optimization of the parameters, the catalyst stability was investigated. Upon completion of each cycle, the catalyst was recovered by centrifugation, washed with hexane and acetone to remove residual products and byproducts, and subsequently dried. To minimize potential losses associated with the transfer, the recovered catalyst was transferred to the reaction vessel as a slurry in acetone, allowing it to dry *in situ* and ensuring minimal variation in the catalyst mass throughout the cycles. The reactions were then performed at the determined optimal conditions of 1 : 24 oil-to-methanol molar ratio, 5 wt% catalyst loading, 150 °C and 1.5 h.

The results showed that the Zn-Gly catalyst could be reused for up to five reaction cycles with no significant loss in activity, as conversions decreased only from 94.5% to 91.7% (Fig. 3e and S7). A decrease in activity for heterogeneous catalysts is usually associated with the leaching or blockage of active sites due to the deposition of byproducts, such as glycerol.[103] However, although the Gly–Zn catalyst indicated no significant loss in performance, PXRD analysis was performed on the spent catalyst to investigate whether its crystalline structure remained intact (Fig. S8). The analysis revealed the appearance of new diffraction peaks at 10.9°, 17.2°, and 20.7°, which are associated with the zinc glycerolate phase. Although the deposition of byproducts on the catalyst surface is expected to affect its activity, Kwong and Yung[104] demonstrated in their study that zinc glycerolate can act as an active site for the transesterification reaction. Therefore, the formation of this new phase explains the sustained catalytic performance of Gly–Zn over five reaction cycles.

FFA effect on catalyst performance

The effect of FFA on Gly–Zn performance was explored by varying the FFA content in the oil used as feedstock. Corn oil was employed as a low-acidity feedstock, while oleic acid was added to the oil at mass ratios ranging from 5 wt% to 50 wt% in order to mimic feedstocks with high FFA content (Fig. 3f and S9).

A conversion of only 4.9% was achieved when corn oil was used as feedstock, while conversions increased significantly as feedstock acidity rose, reaching 88.0% and 94.5% at 5 wt% and 10 wt% FFA, respectively. This performance improvement is likely associated with the formation of zinc oleate, which, according to Kwong *et al.*,[104] acts as a highly active site for transesterification reactions. According to the authors, zinc oleate serves as an intermediate that subsequently reacts with glycerol produced in the reaction media to generate zinc glycerolate, as observed on the surface of the Gly–Zn catalyst.[104]

Moreover, a further increase in acidity to 20 wt% and 50 wt% also led to high catalytic performance, achieving conversion of 93.4% and 87.9%, respectively. Nonetheless, the formation of a white precipitate was observed when reactions were performed using these feedstocks. PXRD and FTIR analyses of the white precipitate identified it as zinc oleate (Fig. S11 and S12), suggesting that the excessive amount of FFA favoured the equilibrium towards the formation of this intermediate, which was not fully converted into zinc glycerolate. Therefore, these findings suggest an overestimation of conversion values, as part of the oleic acid was not converted into biodiesel but consumed to form the zinc oleate.

Considering the sustainable nature of this glycerol-based catalyst, the limitation observed at high acidity levels does not affect the promising outcomes, as the catalyst can still tolerate up to 10 wt% FFA, highlighting its potential for converting unrefined or spent feedstocks.

Reaction mechanism

Based on the surface properties of the catalyst and the formation of zinc oleate as an intermediate and zinc glycerolate confirmed by experimental results, a concerted reaction mechanism as described by Reinoso *et al.*[105] and Kwong *et al.*[104] was proposed.

The mechanism involves first the formation of zinc carboxylates, such as zinc oleate, which act as highly active sites for the

Table 2 Comparative study of the catalytic performance of Gly–Zn with ZnO-based catalysts reported in the literature for biodiesel production

Catalyst	Feedstock	Conditions (molar ratio, catalyst loading, temperature, time)	Conversion (%)	Ref.
MOF/ZnO@CaO	Soybean oil	1 : 40, 5.4 wt%, 25 °C, 0.4 h	92.0	95
ZnO	Sunflower oil	1 : 20, 4.7 wt%, 70 °C, 3 h	71.0	96
ZnO/zeolite	Jatropha oil	1 : 30, 1.0 wt%, 200 °C, 1 h	93.8	97
SrO–ZnO/Al_2O_3	Acidic WCO (18 wt%)	1 : 10 (ethanol), 15 wt%, 75 °C, 5 h	95.7	98
CuO/ZnO	WCO	1 : 9 (ethanol), 5 wt%, 65 °C, 2 h	93.5	99
SO42–/ZnO-β-zeolite	WCO	1 : 15, 3 wt%, 200 °C, 8 h	96.9	100
ZnO-modified starfish	Grapeseed oil	1 : 10, 1 wt%, 68 °C, 10 h	94.7	101
ZnO/Cu-BTC	WCO	1 : 20, 4 wt%, 160 °C, 4 h	92.4	102
Gly–Zn	Acidified corn oil (10 wt%)	1 : 24, 5 wt%, 150 °C, 1.5 h	94.5	This study

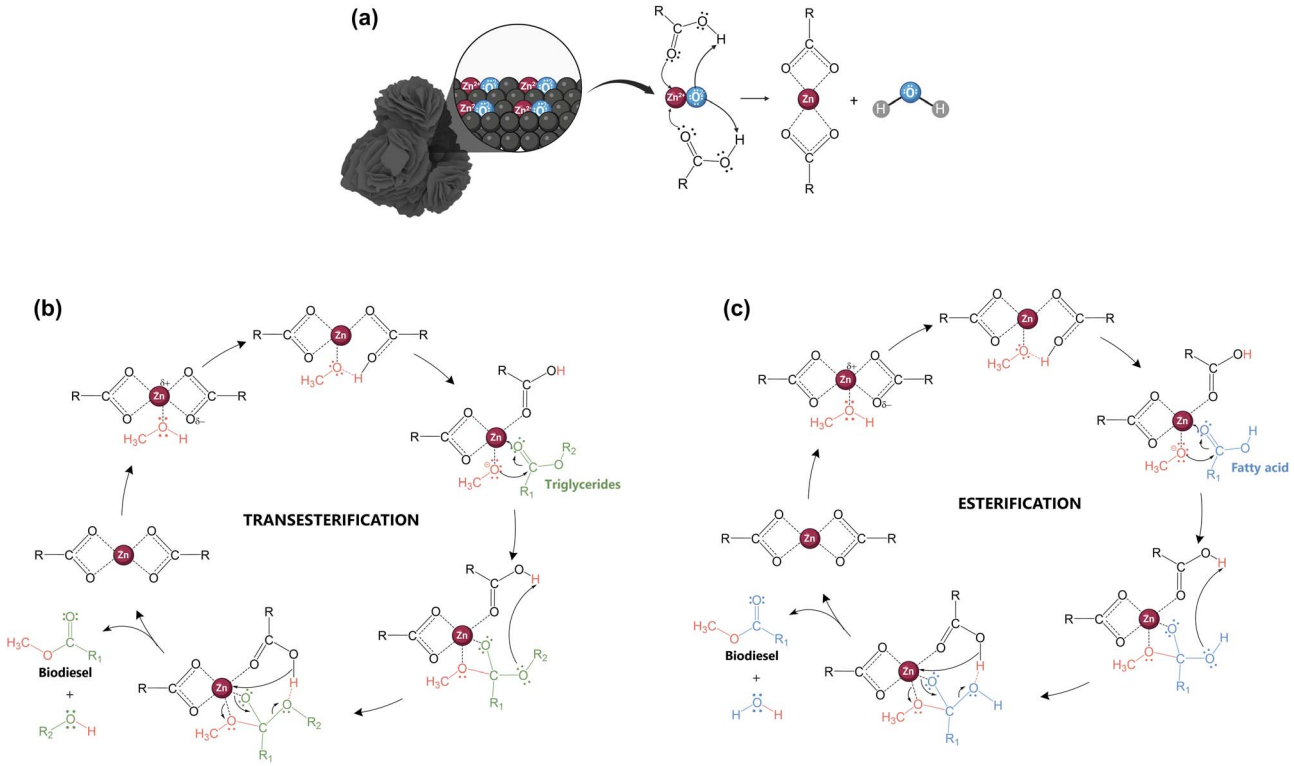

Fig. 4 Proposed mechanism of simultaneous transesterification and esterification using Gly–Zn as a bifunctional catalyst. (a) *In situ* formation of zinc carboxylates active species. (b) Proposed transesterification and (c) esterification mechanism after formation of zinc carboxylate.

transesterification reaction. First, the fatty acid coordinates to the Lewis acidic Zn^{2+} metallic centre through the oxygen of the carboxyl group, while the lattice O^{2-} of the metal oxide acts as the basic sites extracting the proton, through an acid-base reaction, eliminating H_2O and forming the zinc oleate (Fig. 4a).

Subsequently, the most energetically favoured pathway, according to Reinoso *et al.*,[105] for the transesterification, involves the initial coordination of methanol to the Zn^{2+} metal centre of the carboxylate *via* the carboxylate shift, where the carboxylate ligand changes its coordination mode from bidentate to monodentate (Fig. 4b). Thus, it creates a vacant site for methanol adsorption, followed by the co-coordination of the triglyceride. The oxygen from the carboxylate that was previously involved in the bidentate bond captures the proton from methanol, forming the methoxide. Subsequently, the methoxide performs a nucleophilic attack on the carbonyl carbon of the triglyceride, forming a tetrahedral intermediate which undergoes elimination of an alkoxide ion ($^{-}$OR). The eliminated alkoxide ion captures the proton from the carboxylic acid on the catalyst surface, followed by the reestablishment of the bidentate bond of the carboxylate with the metal, regenerating the carboxylate salt and releasing the FAME.

While for the esterification, studies by Reinoso *et al.*[105] also showed that the concerted mechanism is kinetically favoured. The reaction proceeds through similar steps described previously, where methanol and oleic acid co-coordinate to the metallic site *via* the carboxylate shift route (Fig. 4c). The fatty acid coordinates through the carbonyl oxygen, followed by the nucleophilic attack of methoxide into the carbonyl carbon, forming the tetrahedral intermediate. The intermediate undergoes proton exchange, eliminating water and detaching the FAME from the metal site. Moreover, Reinoso *et al.*[105] describes that the glycerol produced during the transesterification acts as a chelating agent on the zinc centre. Thus, glycerol displaces the fatty acid ligands, forming zinc glycerolate, while the coordinated oleic acid is released and subsequently converted into FAME.

Conclusions

A zinc oxide glycerol-based material was successfully synthesized through the carbonization of zinc acetate, urea, and glycerol. The material was comprehensively characterized, confirming the formation of a ZnO-carbon composite with a flower-like morphology, composed of stacked carbon sheets. Textural analysis indicated a mesoporous material, with a surface area of 156.8 $m^2\ g^{-1}$ and a pore diameter of 9.9 nm.

The catalytic efficiency of Gly–Zn was investigated in the conversion of acidified corn oil into biodiesel. Different reaction approaches were investigated, indicating the advantage of the microwave-assisted method, which enhanced reaction rates and conversion. A systematic optimization of the reaction parameters was performed, aiming to achieve the highest biodiesel conversion. A conversion of 94.5% was reached under the conditions of a 1 : 24 oil-to-methanol molar ratio, 5 wt% catalyst loading, 150 °C and 1.5 h. These reaction conditions demonstrate the potential of the microwave-assisted approach, owing to a considerable improvement in the energy requirements.

Reusability tests demonstrated that the material maintained its performance for up to five reaction cycles. This robustness was attributed to the *in situ* formation of zinc glycerolate on the catalyst surface, which acted as an active site for the reactions. These results highlight the potential of heterogeneous glycerol-based catalysts and provide insights into using excess crude glycerol, transforming it into value-added materials, while promoting sustainability and circularity in biodiesel production.

Author contributions

M. P. D.: conceptualization, methodology, investigation, formal analysis, writing – original draft, writing – review and editing; L. P.: investigation, formal analysis, writing – review and editing; T. R. M.: investigation, formal analysis, writing – original draft, writing – review and editing; R. N.: conceptualization, methodology, resources, writing – review and editing, supervision, and funding acquisition.

Conflicts of interest

There are no conflicts to declare.

Data availability

The authors confirm that the data supporting this article have been included as part of the supplementary information (SI). Supplementary information: ^{1}H NMR assignments for canola oil, oleic acid, and biodiesel, ^{1}H NMR spectra of the obtained products, additional PXRD and FTIR analyses. See DOI: https://doi.org/10.1039/d6su00192k.

Acknowledgements

The authors would like to acknowledge funding sources for financial support for this research. RN is grateful to NSERC for funding through the Discovery program and Concordia University for financial support through the Concordia University Research Chair Program. RN also acknowledges the Quebec Centre for Advanced Materials for financial support. MPD is grateful to Concordia University and the Fonds de Recherche du Quebec – Nature et Technologies (https://doi.org/10.69777/344576) for funding through the doctoral scholarship program. LP acknowledges support from Concordia University, the Fonds de Recherche du Quebec – Nature et Technologies (https://doi.org/10.69777/366779), and the Doctoral Studies Abroad Scholarship from the Secretaría Nacional de Ciencia, Tecnología e Humanidades (Mexico). The authors are also grateful to Ms. Clara Vieira for her assistance with the N_2 adsorption and desorption analysis. Fig. 2, and the Table of Contents were created in BioRender (https://BioRender.com/dsqpyl1, https://BioRender.com/p16wla1).

References

1 M. J. B. Kabeyi and O. A. Olanrewaju, *Front. Energy Res.*, 2022, **9**, 743114.
2 J. Wang and W. Azam, *Geosci. Front.*, 2024, **15**, 101757.
3 M. Ali Ijaz Malik, S. Zeeshan, M. Khubaib, A. Ikram, F. Hussain, H. Yassin and A. Qazi, *Energy Convers. Manag:x*, 2024, **23**, 100675.
4 IEA, *Global Energy Review 2025*, Paris, 2025.
5 M. Kelkar, *Heliyon*, 2024, **10**, e39200.
6 R. Nehring, *Philos. Trans. R. Soc. Lond. B Biol. Sci.*, 2009, **364**, 3067–3079.
7 C. W. Schmidt, *Environ. Health Perspect.*, 2007, **115**, A86.
8 S. I. S. Mohammad, A. Vasudevan, K. D. V. Prasad, I. R. Ali, A. Kumar, A. Kulshreshta, V. S. Mann, I. B. Sapaev, T. Kalyani and M. Sina, *Heliyon*, 2025, **11**, e41416.
9 E. P. Venkatesan, R. Krishnaiah, K. Prasad, S. R. Medapati, S. R. Sree, M. Asif, S. A. Khan and E. Linul, *ACS Omega*, 2024, **9**, 6709–6718.
10 M. A. Fazal, A. S. M. A. Haseeb and H. H. Masjuki, *Renew. Sustain. Energy Rev.*, 2011, **15**, 1314–1324.
11 J. C. Pasqualino, D. Montané and J. Salvadó, *Biomass Bioenergy*, 2006, **30**, 874–879.
12 M. P. Dorado, E. Ballesteros, J. M. Arnal, J. Gómez and F. J. López, *Fuel*, 2003, **82**, 1311–1315.
13 M. P. Duarte and R. Naccache, *Catal. Sci. Technol.*, 2024, **14**, 3864–3877.
14 I. M. Atadashi, M. K. Aroua, A. R. Abdul Aziz and N. M. N. Sulaiman, *J. Ind. Eng. Chem.*, 2013, **19**, 14–26.
15 B. Changmai, C. Vanlalveni, A. P. Ingle and R. Bhagat, *RSC Adv.*, 2020, **10**, 41625.
16 M. Abdul, H. Shaah, M. Sohrab Hossain, F. Aboelksim, S. Allafi, A. Alsaedi, N. Ismail, M. Omar, A. Kadir and M. I. Ahmad, *RSC Adv.*, 2021, **11**, 25018–25037.
17 V. Mandari and K. S. Devarai, *Bioenergy Res.*, 2022, **15**, 935–961.
18 Y. C. Sharma, B. Singh and J. Korstad, *Fuel*, 2011, **90**, 1309–1324.
19 F. E. Kiss, M. Jovanović and G. C. Bošković, *Fuel Process. Technol.*, 2010, **91**, 1316–1320.
20 L. Du, Z. Li, S. Ding, C. Chen, S. Qu, W. Yi, J. Lu and J. Ding, *Fuel*, 2019, **258**, 116122.
21 B. Gurunathan and A. Ravi, *Bioresour. Technol.*, 2015, **188**, 124–127.
22 Z. Li, S. Ding, C. Chen, S. Qu, L. Du, J. Lu and J. Ding, *Energy Convers. Manag.*, 2019, **192**, 335–345.
23 A. M. Doyle, T. M. Albayati, A. S. Abbas and Z. T. Alismaeel, *Renewable Energy*, 2016, **97**, 19–23.
24 A. Macina, T. V. de Medeiros and R. Naccache, *J. Mater. Chem. A Mater.*, 2019, **7**, 23794–23802.
25 M. C. Nongbe, T. Ekou, L. Ekou, K. B. Yao, E. Le Grognec and F. X. Felpin, *Renewable Energy*, 2017, **106**, 135–141.
26 P. Karuppiah Subramanian and P. Muthiah, *Environ. Prog. Sustain. Energy*, 2016, **35**, 308–314.
27 Y. C. Lin, K. T. T. Amesho, C. E. Chen, P. C. Cheng and F. C. Chou, *Sustain. Chem. Pharm.*, 2020, **17**, 100310.

28 B. Maleki, S. S. Ashraf Talesh and M. Mansouri, *Mater. Today Sustain.*, 2022, **18**, 100157.
29 W. Xie and H. Wang, *J. Ind. Eng. Chem.*, 2020, **87**, 162–172.
30 W. Xie and H. Wang, *Renewable Energy*, 2020, **145**, 1709–1719.
31 W. Xie, C. Gao and J. Li, *Renewable Energy*, 2021, **168**, 927–937.
32 S. Yan, S. O. Salley and K. Y. Simon Ng, *Appl. Catal. A Gen.*, 2009, **353**, 203–212.
33 M. F. Rabiah Nizah, Y. H. Taufiq-Yap, U. Rashid, S. H. Teo, Z. A. Shajaratun Nur and A. Islam, *Energy Convers. Manag.*, 2014, **88**, 1257–1262.
34 Y. Zhang, S. Niu, S. Xia, S. Liu and J. Liu, *Renewable Energy*, 2023, **217**, 119139.
35 W. Meka Kedir, in *Advanced Biodiesel - Technological Advances, Challenges, and Sustainability Considerations*, IntechOpen, 2024.
36 A. Munyentwali, H. Li and Q. Yang, *Appl. Catal. A Gen.*, 2022, **633**, 118525.
37 H. Pan, Q. Xia, Y. Wang, Z. Shen, H. Huang, Z. Ge, X. Li, J. He, X. Wang, L. Li and Y. Wang, *Fuel Process. Technol.*, 2022, **237**, 107421.
38 J. I. Orege, O. Oderinde, G. A. Kifle, A. A. Ibikunle, S. A. Raheem, O. Ejeromedoghene, E. S. Okeke, O. M. Olukowi, O. B. Orege, E. O. Fagbohun, T. O. Ogundipe, E. P. Avor, O. O. Ajayi and M. O. Daramola, *Energy Convers. Manag.*, 2022, **258**, 115406.
39 R. Leesing, S. Siwina and K. Fiala, *Renewable Energy*, 2021, **171**, 647–657.
40 T. V. de Medeiros, A. Macina and R. Naccache, *Nano Energy*, 2020, **78**, 105306.
41 S. H. Y. S. Abdullah, N. H. M. Hanapi, A. Azid, R. Umar, H. Juahir, H. Khatoon and A. Endut, *Renew. Sustain. Energy Rev.*, 2017, **70**, 1040–1051.
42 C. E. Akhabue, E. O. Osa-Benedict, E. A. Oyedoh and S. K. Otoikhian, *Renewable Energy*, 2020, **152**, 724–735.
43 A. M. Shobhana-Gnanaserkhar, N. Asikin-Mijan, G. AbdulKareem-Alsultan, S. Seenivasagam, S. M. Izham and Y. H. Taufiq-Yap, *Biomass Bioenergy*, 2020, **141**, 105714.
44 B. Maleki, Y. Kalanakoppal Venkatesh, S. Siamak Ashraf Talesh, H. Esmaeili, S. Mohan and G. R. Balakrishna, *Chem. Eng. J.*, 2023, **467**, 143399.
45 C. R. Chilakamarry, A. M. M. Sakinah, A. W. Zularisam and A. Pandey, *Syst. Microbiol. Biomanuf.*, 2021, **1**, 378–396.
46 C. H. Zhou, J. N. Beltramini and G. Q. Lu, *Chem. Soc. Rev.*, 2008, **37**, 527–549.
47 B. L. A. P. Devi, K. N. Gangadhar, P. S. S. Prasad, B. Jagannadh and R. B. N. Prasad, *ChemSusChem*, 2009, **2**, 617–620.
48 B. Hazmi, M. Beygisangchin, U. Rashid, W. N. A. W. Mokhtar, T. Tsubota, A. Alsalme and C. Ngamcharussrivichai, *Molecules*, 2022, **27**, 7142.
49 J. Starvaggi and R. Ettari, *Pharmaceuticals*, 2025, **18**, 1692.
50 T. V. De Medeiros, J. Manioudakis, F. Noun, J. R. Macairan, F. Victoria and R. Naccache, *J. Mater. Chem. C Mater.*, 2019, **7**, 7175–7195.
51 A. S. I. Ibrahim, H. Boyaci, B. Gözmen and Ö. Sönmez, *Biomass Bioenergy*, 2026, **206**, 108630.
52 A. S. I. Ibrahim, B. Gözmen and Ö. Sönmez, *Fuel*, 2024, **371**, 131988.
53 E. Demir, S. D. Çalhan and Ö. Sönmez, *Biomass Bioenergy*, 2025, **201**, 108148.
54 A. Kavlak and Ö. Sönmez, *Biofuels*, 2023, **14**, 137–146.
55 D. Wang, Z. Pan, G. Chen and Z. Lu, *Electrochim. Acta*, 2021, **379**, 138170.
56 I. Adolfo Lutz, in *Métodos físicos-quimicos para análise de Alimentos*, ed. O. Zenebon, N. S. Pascuet and P. Tiglea, Instituto Adolfo Lutz, São Paulo, IV, 2008, pp. 595–596.
57 M. A Alotaibi, A. Naeem, I. Wali Khan, M. Farooq, I. Ud Din and M. S. Saharun, *Biomass Bioenergy*, 2024, **182**, 107078.
58 M. Tariq, S. Ali, F. Ahmad, M. Ahmad, M. Zafar, N. Khalid and M. A. Khan, *Fuel Process. Technol.*, 2011, **92**, 336–341.
59 Y. Chang, M. Antonietti and T. P. Fellinger, *Angew. Chem., Int. Ed.*, 2015, **54**, 5507–5512.
60 Z.-Y. Wu, S.-L. Xu, Q.-Q. Yan, Z.-Q. Chen, Y.-W. Ding, C. Li, H.-W. Liang and S.-H. Yu, *Sci. Adv.*, 2018, **4**, 788–815.
61 A. Rokade, G. K. Rahane, A. Živković, S. N. Rahane, H. S. Tarkas, K. Hareesh, N. H. de Leeuw, S. D. Sartale, N. Y. Dzade, S. R. Jadkar and S. R. Rondiya, *Langmuir*, 2024, **40**, 6884–6897.
62 Y. C. Chang, C. H. Huang and W. R. Liu, *Polymers*, 2022, **14**, 3085.
63 I. M. Mendonça, O. A. R. L. Paes, P. J. S. Maia, M. P. Souza, R. A. Almeida, C. C. Silva, S. Duvoisin and F. A. de Freitas, *Renewable Energy*, 2019, **130**, 103–110.
64 L. Lorenzini, M. G. Anunciação, I. B. Gomes, R. C. F. Silva, T. A. Silva, R. P. L. Moreira, P. S. Pinto and A. P. C. Teixeira, *Int. J. Hydrogen Energy*, 2025, **135**, 382–392.
65 M. H. Suhag, A. Khatun, I. Tateishi, M. Furukawa, H. Katsumata and S. Kaneco, *ACS Omega*, 2023, **8**, 11824–11836.
66 M. Thommes, K. Kaneko, A. V. Neimark, J. P. Olivier, F. Rodriguez-Reinoso, J. Rouquerol and K. S. W. Sing, *Pure Appl. Chem.*, 2015, **87**, 1051–1069.
67 H. B. W. Patterson, *Bleaching and Purifying Fats and Oils: Theory and Practice*, 2009, pp. 1–52.
68 H. Xu, X. Ye, X. Shi, H. Zhong, D. He, B. Jin and F. Jin, *Mol. Catal.*, 2022, **522**, 112241.
69 A. Nagvenkar, S. Naik and J. Fernandes, *Catal. Commun.*, 2015, **65**, 20–23.
70 S. Mahala, S. M. Arumugam, S. Kumar, B. Devi and S. Elumalai, *Nanoscale Adv.*, 2023, **5**, 2470.
71 M. Xia, S. Zhang, Y. Cai, L. Deng, X. Wang, J. Wan, Y. Liu, C. Tan, R. P. Singh and G. Wu, *ACS Appl. Mater. Interfaces*, 2026, **18**, 24632–24647.
72 K. Vankudoth, A. H. Padmasri, R. Sarkari, V. K. Velisoju, N. Gutta, N. K. Sathu, C. N. Rohita and V. Akula, *New J. Chem.*, 2017, **41**, 9875–9883.
73 P. Du, T. Su, X. Luo, X. Xie, Z. Qin and H. Ji, *Catalysts*, 2019, **9**, 716.
74 S. Lee, J. Ha and O. L. Li, *Nanomaterials*, 2024, **14**, 1313.

75 P. Wang, S. Hou, H. Gou, F. Guo, M. Wang, T. Wang, J. Liu, J. Tao, H. Pan and J. Ni, *Int. J. Hydrogen Energy*, 2025, **135**, 104–110.
76 A. Wang, W. Quan, H. Zhang, H. Li and S. Yang, *RSC Adv.*, 2021, **11**, 20465–20478.
77 D. Rhithuparna, N. Ghosh, S. Lalthazuala Rokhum and G. Halder, *Chem. Eng. J.*, 2024, **482**, 149033.
78 F. Motasemi and F. N. Ani, *Renew. Sustain. Energy Rev.*, 2012, **16**, 4719–4733.
79 Y. Huo, S. Xiu, L. Y. Meng and B. Quan, *Chem. Eng. J.*, 2023, **451**, 138572.
80 M. C. M. D. de Conti, S. Dey, W. E. Pottker and F. A. La Porta, *Mater. Today Sustain.*, 2023, **23**, 100458.
81 I. Thushari, S. Babel and C. Samart, *Renewable Energy*, 2019, **134**, 125–134.
82 M. Athar and S. Zaidi, *J. Environ. Chem. Eng.*, 2020, **8**, 104523.
83 B. Khedri, M. Mostafaei and S. M. Safieddin Ardebili, *Energy Sources, Part A Recovery, Util. Environ. Eff.*, 2019, **41**, 2377–2395.
84 D. T. Oyekunle, M. Barasa, E. A. Gendy and S. K. Tiong, *Process Saf. Environ. Prot.*, 2023, **177**, 844–867.
85 M. Marinković, H. Waisi, S. Blagojević, A. Zarubica, R. Ljupković, A. Krstić and B. Janković, *Fuel*, 2022, **315**, 123246.
86 P. Verma and M. P. Sharma, *Renew. Sustain. Energy Rev.*, 2016, **62**, 1063–1071.
87 N. S. Topare, R. I. Jogdand, H. P. Shinde, R. S. More, A. Khan and A. M. Asiri, *Mater. Today Proc.*, 2022, **57**, 1605–1612.
88 B. Changmai, M. Van Lal Chhandama, C. Vanlalveni, A. E. H. Wheatley and S. L. Rokhum, in *Biodiesel Production: Feedstocks, Catalysts, and Technologies*, eds. S. L. Rokhum, G. Halder, S. Assabumrungrat and K. Ngaosuwan, John Wiley & Sons Ltd, 1st edn, 2022, pp. 209–227.
89 V. Enguilo Gonzaga, R. Romero, R. M. Gómez-Espinosa, A. Romero, S. L. Martínez and R. Natividad, *ACS Omega*, 2021, **6**, 24092–24105.
90 R. Ihsan, A. Naeem, M. Farooq, T. Saeed, M. Noman, G. Abid and T. Malik, *Renewable Energy*, 2025, **238**, 121939.
91 Q. Shu, J. Gao, Z. Nawaz, Y. Liao, D. Wang and J. Wang, *Appl. Energy*, 2010, **87**, 2589–2596.
92 A. Wang, H. Li, H. Zhang, H. Pan and S. Yang, *Materials*, 2018, **12**, 83.
93 N. M. Alahmar, N. I. B. W. Azelee and S. Toemen, *Sci. Rep.*, 2025, **15**, 352.
94 M. A. Gonçalves, H. C. Lima dos Santos, P. M. Melo da Silva, A. Paula da Luz Corrêa, T. S. Ribeiro, I. de Araújo Sobrinho, G. Narciso da Rocha Filho and L. R. Vieira da Conceição, *RSC Adv.*, 2024, **14**, 20743–20756.
95 M. Sharifi, S. Tangestaninejad, M. Moghadam, A. Marandi, V. Mirkhani, I. Mohammadpoor-Baltork and S. Aghayani, *Sci. Rep.*, 2025, **15**, 3610.
96 S. M. Salim, R. Izriq, M. M. Almaky and A. A. Al-Abbassi, *Fuel*, 2022, **321**, 124135.
97 D. Singh, R. Bhoi, A. Ganesh and S. Mahajani, *Energy Fuels*, 2014, **28**, 2743–2753.
98 A. Al-Saadi, B. Mathan and Y. He, *Chem. Eng. Res. Des.*, 2020, **162**, 238–248.
99 M. Guo, W. Jiang, J. Ding and J. Lu, *Fuel*, 2022, **315**, 123254.
100 B. O. Yusuf, S. A. Oladepo and S. A. Ganiyu, *ACS Omega*, 2023, **8**, 23720–23732.
101 J. Ha, S. Lee and O. L. Li, *Catalysts*, 2025, **15**, 372.
102 B. O. Yusuf, S. A. Ganiyu, A. M. P. Peedikakkal and S. A. Oladepo, *Biomass Bioenergy*, 2026, **204**, 108381.
103 J. Zhu, S. Niu, A. Abulizi, Y. Xu, X. Li, Y. Zheng, Y. Wei, Y. Zhang, Y. Hao, S. Liu, J. Liu and Z. Yang, *Renewable Energy*, 2025, **249**, 123300.
104 T. L. Kwong and K. F. Yung, *Renewable Energy*, 2016, **90**, 450–457.
105 D. M. Reinoso, M. L. Ferreira and G. M. Tonetto, *J. Mol. Catal. A Chem.*, 2013, **377**, 29–41.

